Analyst

Accepted Manuscript

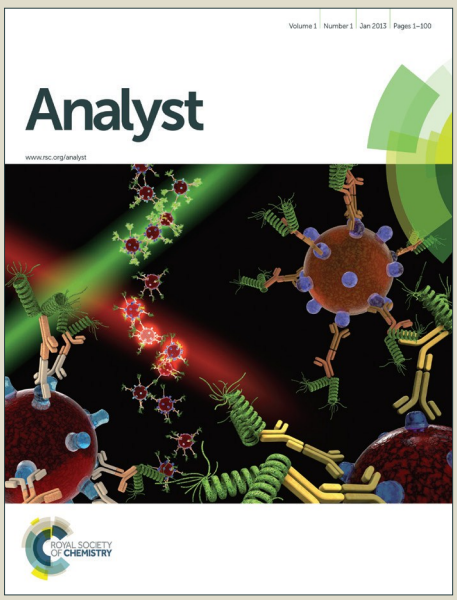

ROYAL SOCIETY OF CHEMISTRY

www.rsc.org/analyst

Journal Name

ARTICLE

Self-Assembled Biosensor with Universal Reporter and Dual-Quenchers for Detection of Unlabelled Nucleic Acids†

Received 00th January 20xx,
Accepted 00th January 20xx

DOI: 10.1039/x0xx00000x

www.rsc.org/

Liming Huang*[a], Gyan H. Aryal, Suk-Wah Tam-Chang*[a], Nelson G. Publicover[a], and Kenneth W. Hunter[a]

A novel biosensor with universal reporter and dual quenchers was developed for rapid, sensitive, selective, and inexpensive detection of unlabelled nucleic acids. The biosensor is based on a single-strand DNA stem-loop motif with an extended universal reporter-binding region, a G-base rich stem region, and a universal address-binding region. The self-assembly of these stem-loop probes with fluorescence labeled universal reporter and a universal address region conjugated to gold nanoparticles forms the basis of a biosensor for DNA or microRNA targets in solution. The introduction of dual quenchers (G-base quenching and gold surface plasmon resonance–induced quenching) significantly reduces the fluorescence background to as low as 12% of its original fluorescence intensity and hence enhances the detection limit to 0.01 picomoles without signal ampilication.

Introduction

Detection of nucleic acids plays a very important role in clinical diagnostics, biological research, environmental monitoring, and homeland security.[1-4] Recently, the development of simple, rapid, sensitive, and selective biosensors for detecting nucleic acids has been actively pursued by many different research groups. Among them, biosensors based on molecular beacons (MB) allow real-time detection of unlabelled nucleic acids in solutions and in cells.[5-8] MB are single-stranded oligonucleotides that form hairpin-shaped stem-loop structures through self-hybridization. A fluorophore is covalently labelled on one end of the oligonucleotide and a non-fluorescent quencher is attached to the other end. In the absence of a target nucleic acid, the hairpin structure brings the fluorophore and the quencher in close proximity, causing the fluorescence of the fluorophore to be quenched. Upon the addition of a target sequence, the MB undergoes a conformational change with the stem opening that results in restoration of fluorescence (Figure 1).[9,10] The hairpin-shaped structure of MBs affords high sequence-specificity and sensitivity.[10] Since its first introduction in 1996, MBs have been widely used in many different areas such as genomics, real-time PCR, and for the detection of proteins and microRNA within living cells.[10-15]

A conventional MB employs an organic dye as a fluorescence reporter and an organic non-fluorescent molecule as a quencher. For detecting each specific target sequence, a MB needs to be doubly labelled with a fluorophore and a quencher, thus suffering from problems such as tedious synthetic process, low synthetic yield, and high cost. For detecting hundreds or thousands of target sequences including microRNAs using the MB technique, the cost is substantial. Many attempts have been made to simplify the synthetic process for the construction of MB by modifying a quencher with metal nanoquenchers such as gold and silver nanoparticles.[16-19] These metal-based nanomaterials exhibit great quenching properties, thereby improving detection sensitivity. However they are still expensive to synthesize, especially for the analysis of many different target sequences of interest. Other researchers have made attempts to develop economical synthetic methods, such as using carbon nanomaterials (e.g. carbon nanotubes and graphene) as quenchers with easy modification on the surface through non-covalent π-π interactions.[20-22] However, the lack of controllability in their size and functional groups on the surface of these nanomaterials has limited reproducibility in biological applications.

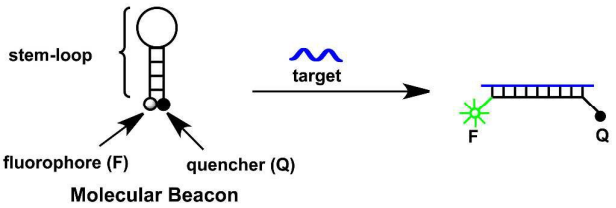

Figure 1. Molecular Beacon.

In response to these limitations, we have developed a self-assembled biosensor for detecting DNA and microRNA target sequences called the stem-loop probe (SP) with universal reporter (UR). As shown in Figure 2a, SP is a single-stranded oligonucleotide designed for detecting a specific target sequence of interest. It forms a hairpin-like structure with a stem region and a loop region that are complementary to a

[a] Department of Microbiology and Immunology, School of Medicine, University of Nevada, Reno, NV 89557, USA, E-mail: huang@medicine.nevada.edu
† Electronic Supplementary Information (ESI) available. See
DOI: 10.1039/x0xx00000x

nucleic acid target. However, unlike a conventional MB labelled on each end with a fluorophore and a quencher, one end of the SP has an extended reporter binding region that is complementary to a single-stranded, fluorophore-labelled UR. The other end of the SP has an extended universal address-binding region that allows self-assembly with gold nanoparticles (AuNP) modified with a universal address region (UADD-AuNP). These two regions remain unchanged for all targets of interest. In the stem region, multiple G bases were specially designed not only to stabilize the hairpin structure, but also serve as fluorescence quenchers.[23] For the detection of different target sequences, only the stem and loop region on SP need to be modified for capturing the target sequences. The fluorescent dye tetramethylrhodamine (TAMRA) was selected to label the universal reporter strand because the fluorescence of TAMRA can be selectively quenched by G-bases through an electron-transfer mechanism.[23,24] The fluorescence quenching of TAMRA is dependent upon the distance between the fluorophore and the G bases, and the number of G bases as well. UADD is a complementary strand to the address-binding region of SP, thus UADD conjugated AuNPs can be linked to SP by hybridization. AuNPs serve as secondary quenchers based on a gold surface plasmon resonance–induced quenching mechanism that enhances quenching efficiency, lowers fluorescence background, and thus increases sensitivity.[25,26] A complex sensing structure, UR-SP-UADD-AuNPs is formed after the self-assembly of mixed components of SP, UR, and UADD-AuNPs after a heating and cooling process in solution. Before the addition of a target nucleic acid, SP is locked in the hairpin-closed form where the fluorophore is in close proximity to G bases on the SP stem region and the gold surface, and the fluorescent emission is strongly quenched (Figure 2b). After the addition of a target nucleic acid, the SP changes its conformation to the hairpin-opened form. The fluorophore is no longer in close proximity to the quenchers and restoration of fluorescence emission signals the presence of the target (Figure 2c). To construct biosensors for detecting different target sequences, only SP needs to be modified; UR and UADD remain the same. As an example shown in Table S1,† the bulk custom synthesis of UR and UADD for detecting a large number of targets of interest could reduce by the cost as much as 90% compared to the cost for dual-labelled MB.

Chemicals and materials

Thioacetic acid was purchased from Sigma-Aldrich and used without further purification. Gold nanoparticles in aqueous solution (10 nm diameter, 0.01 wt%, 5.7×10^{12} particles/mL ≈ 9.5×10^{-9} M) were purchased from Nanocs, Inc. (New York). All oligonucleotides used in the studies were custom synthesized by Integrated DNA Technologies, Inc. (IDT). The buffer solutions used in the study are as follows: Operating buffer (B1, pH 7.4) for conducting all fluorescence studies contains 11.9 mM phosphate, 137 mM NaCl, 5 mM Mg^{2+} and 2.7 mM KCl; The hybridization buffer (B2, pH 7.4, it is similar to buffer B1 but without addition of Mg^{2+}) was diluted from a 10x concentrated PBS buffer solution purchased from Fisher Scientific. The washing buffer (B3, pH 7.0) contains 10 mM phosphate and 300 mM NaCl. Stock solutions of oligonucleotides were prepared by dissolving oligonucleotides in B2 buffer in the receiving tubes. In general, stock solutions of approximately 10^{-3} M or 10^{-4} M were prepared and kept in a freezer at -20 °C.

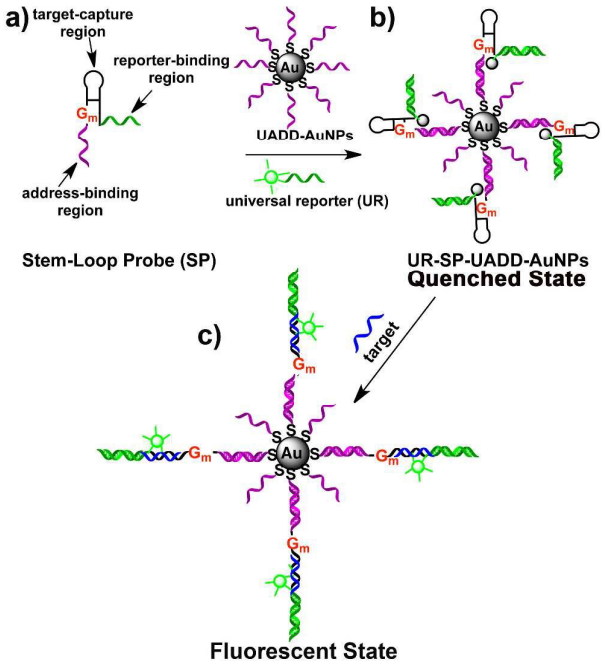

Figure 2. Schematic illustration of the self-assembly of UR-SP-UADD-AuNPs biosensors and the detection of unlabelled nucleic acid targets. (a) A stem-loop probe (SP); (b) Self-assembled UR-SP-UADD-AuNPs (quenched state); and (c) SPs in the opened form (fluorescent state) in the presence of unlabelled oligonucleotide targets.

Experimental

Instrumentation: A Jouan MR23i centrifuge was used for separating gold nanoparticles from aqueous solutions. Absorption spectra were obtained using a dual-beam Perkin Elmer Lambda 950 spectrophotometer with software UV-WIN Lab (version 5.1.5). Fluorescence spectra were acquired using a Jobin-Yvon Horiba Fluorolog 3-222 spectrophotometer with FluorEssence software. Cuvettes with 1 mL volume loading capacity and 5-mm path length (mini-cuvette) or 50 µL volume loading capacity and 10-mm path length (micro-cuvette) (purchased from Starna, CA, USA) were used in the studies to minimize the consumption of DNA or microRNA solutions.

Preparation of universal address oligonucleotide conjugated gold nanoparticles (UADD-AuNPs): The preparation of UADD-AuNPs followed a modified procedure.[27] In a typical preparation, disulfide-functionalized universal address oligonucleotide (UADD: 5' C6SS-CTC TCC CTC CCT CCC TCC C-3') solution (20 µL, 100 µM) was added to a 600 µL AuNPs solution in a 1.5-mL plastic tube. NaCl (5 µL, 5 M) and Na_2HPO_4 (50 µL, 50 mM, pH 7.0) were then added, and the mixture was incubated at room temperature for 24 h. Then NaCl (5 µL, 5 M) and Na_2HPO_4 (50 µL, 50 mM, pH 7.0) were added again and the mixture was further incubated at 40 °C for 12 hours. In order to increase the ionic strength of the solution gradually,

NaCl (5 µL, 5 M) was added every 12 hours over the next 48 hours while the mixture was incubated at 40 °C. This step replaces a vacuum centrifugation to give stable nanoparticles and increase the coverage of oligonucleotides on the surface of AuNPs. Excess unbound universal address oligonucleotides were removed by centrifugation (14000 RPM, 20 minutes) and suspension of AuNPs in 100 µL B3 buffer four times. The final UADD-AuNPs were suspended in a B2 buffer solution (600 µL) and stored at 4 °C.

Determination of the coverage of UADD oligonucleotides on AuNPs: The coverage of UADD olionucleotides on Au nanoparticles was estimated using a fluorophore (Alexa-488, λ_{ex} = 488 nm) labelled UADD (Alexa-UADD: 5' C6SS-CTC TCC CTC CCT CCC TCC C-Alexa 3') using UV-vis and fluorescence spectroscopy. Alexa-UADD-AuNPs were prepared together with UADD-AuNPs using the same procedure in parallel. The concentration of recovered AuNPs in an Alexa-UADD-AuNPs solution after surface modification was estimated by comparing the UV-vis λ_{max} (520-530 nm) with the fresh AuNPs sample. As shown in Figure S1,† the absorption spectrum of Alexa-UADD-AuNPs almost overlaps with that of the fresh AuNPs solution, suggesting a complete recovery (~100%) of AuNPs, thus the concentration of Alexa-UADD capped AuNPs is about $9.5x10^{-9}$ M. The total concentration of Alexa-UADD oligonucleotides immobilized on the AuNPs is calculated based on the fluorescence intensity of free Alexa-UADD after displacement. To displace Alexa-UADD oligonucleotides from AuNPs, a large excess mercaptoacetic acid solution (6 µL, 0.1 M) was added into 594 µL of a diluted Alexa-UADD-AuNPs solution (60 times dilution from the original solution).[28] After 18 hours, a solution with free Alexa-UADD oligonucleotides was separated from gold aggregates by centrifugation and the fluorescence intensity of Alexa-UADD in the solution was measured and compared with standard solutions of Alexa-UADD. The concentration of Alexa-UADD in the diluted Alexa-UADD-AuNPs solution was calculated to be $7.6x10^{-9}$ M after comparing its fluorescence intensity with that of an Alexa-UADD standard solution (10 nM), and the concentration of Alexa-UADD in the concentrated solution was calculated to be $4.56x10^{-7}$ M. Alexa-UADD oligonucleotides immobilized on each Au nanoparticle was calculated to be 48±2 per particle based on three trials. We anticipate the number of UADD oligonucleotides immobilized on each Au nanoparticle is similar to that of Alexa-UADD because of the similarity of UADD and Alexa-UADD, especially because they both use same oligonucleotide sequences and same disulfide functional groups.

The self-assembly of the universal reporter, stem-loop probe and UADD-AuNPs: A solution of the universal reporter (2 µL, 100 µM) and a solution of stem-loop probe (1 µL, 100 µM) were added to a solution of UADD-AuNPs (100 µL, ~$9.5x10^{-9}$ M particles) in a 200-µL plastic tube. The mixture was heated to 80 °C and kept for 10 minutes using a thermomixer (Eppendorf Thermomixer R, Brinkmann Instruments, Inc.). Then it was cooled down to 25 °C slowly. The excess free universal reporter and stem-loop probe oligonucleotides were removed by three cycles of centrifugation (14000 RPM, 20 minutes) and suspension of the particles in B2 buffer. Finally, UR-SP-UADD-AuNPs were re-suspended in 100 µL of B2 buffer and stored at 4 °C.

Determination of the loading of UADD-AuNPs with UR-SP probes: The loading of universal address conjugated particles with UR-SP probes was determined using UV-vis and fluorescence spectroscopy. In a typical experiment, 600 µL of a diluted solution of UR-SP-UADD-AuNPs (60 times dilution from the stock solution described above) was heated to 76 °C in a 1-mL fluorescence cuvette and the fluorescence of the solution was recorded when UR, SP, and UADD-AuNPs were dehybridized completely. A standard solution containing 5 and 10 nM of UR-SP-ADD (1:1:1) as standard solutions was heated to 76 °C and the fluorescence spectra of the solutions were recorded. The concentration of UR-SP loaded on UADD-AuNPs in the diluted solution was calculated by comparison with the standard solution to be 3.5 nM, thus, the concentration of UR-SP loaded on UADD-AuNPs in the stock solution was 210 nM.

Table 1. Abbreviations and sequences of oligonucleotides used in the study (5'-3')

UR	TAMRA-linker-AAA ATA ACC ACC CAC CCA CCC	*T_m= 61.9 °C, 66.2 °C (100 nM)
UADD	C6SS-CTC TCC CTC CCT CCC TCC C	*T_m= 62.8 °C
Alexa-UADD	C6SS-CTCTCCCTCCCTCCCTCCC-Alexa	
SP1	GGG TGG GTG GGT GGT TAT TTT CCC TTA CAT CGT GGG TGC TTC CGT AAG GGT GGG AGG GAG GGA GGG AGA G	*#T_m= 61.5 °C
SP2	GGG TGG GTG GGT GGT TAT TTT CCC TAA CCC ATG GAA TTC AGT TCT TAG GGA GGG AGG GAG GGA GGG AGA G	*#T_m= 46.1 °C
T1.1	CTT ACG GAA GCA CCC ACG ATG	*T_m= 62.0 °C
T1.2	GGA AGC ACC CAC GAT	*T_m= 54.0 °C
T1.3	GGA AGA ACC CAC GAT	*&T_m= 43.3 °C
T1.4	rCrUrU rArCrG rGrArA rGrCrA rCrCrC rArCrG rArUrG	*T_m= 60.4 °C
T1.5	AGT CAA TCT GTG TTG TGA GCC G	
T2.1	TG AGA ACT GAA TTC CAT GGG TT	*T_m= 53.5 °C
T2.2	rUrG rArGrA rArCrU rGrArA rUrUrC rCrArU rGrGrG rUrU	*T_m= 53.8 °C

* The melting temperatures were calculated using an OligoAnalyzer 3.1 program based on 5 nM of oligonucleotides in the buffers containing 137 mM NaCl and 5 mM Mg^{2+}. In addition, the melting temperature of UR with a concentration of 100 nM was calculated in order to compare with the experiment result.

This is the melting temperature of the primary hairpin structure of SP.

& This is the melting temperature of the T1.3 with single base mismatch.

(The OligoAnalyzer 3.1 program is available on www.idtdna.com)

The concentration of particles in the stock solution was estimated by UV-vis spectroscopy to be 7.2 nM. The number of UR-SP hybridized on each UADD-AuNP particle was calculated to be 29±1 per nanoparticle with three trials and the loading capability of UR-SP on UADD-AuNPs was estimated to be ~60% with respect to the number of UADD (48± 2 per particle) on each AuNP estimated above.

Detection of target sequences using self-assembled UR-SP-UADD-AuNPs: In a typical assay, a target solution was added into UR-SP-UADD-AuNPs solution (5 nM of UR-SP and 0.17 nM of AuNPs in buffer B1). The mixed solutions were incubated at 37 °C for 20 minutes and cooled down to 25 °C in a thermomixer (Eppendorf Thermomixer R, Brinkmann Instruments, Inc.). The emission spectra of the UR-SP-UADD-AuNPs solutions were recorded at 25 °C before and after incubation of a target.

Results and discussion

To demonstrate the principle of this newly designed self-assembled biosensor for detection of specific target nucleic acids, the oligonucleotides listed in Table 1 were designed taking into consideration their calculated melting temperatures. UR (TAMRA-linker-AAA ATA ACC CAC CCA CCC) and UADD (C6SS-CTC TCC CTC CCT CCC TCC C) are universal sequences designed for all target sequences of interest and were synthesized in bulk. They both have an approximate melting temperature greater than 60 °C to ensure complete hybridization with SP at room temperature or 37 °C. The thermal denaturation experiment of UR (100 nM) has suggested a melting temperature of 67.9 °C which is slightly higher than the calculated value (66.2 °C) (Figure S6†). In order to demonstrate the universality of the system, two stem-loop probes corresponding to two different target sequences were designed. SP1 contains a target capture region that matches a target sequence T1.1 that is a segment of the murine B7.2 mRNA sequence (NCBI L25606).[29] T1.2, T1.3, T1.4, and T1.5 are complementary strands of the loop region, a single base mismatch, the RNA form of T1.1, and a complete mismatch, respectively. SP2 contains a target capture region matching with a target DNA sequence T2.1 and microRNA sequence T2.2 that is a segment of microRNA-146a.[30] The biosensor was constructed using the procedure described in the experimental section above. In brief, disulfide functionalized UADD sequences were immobilized on AuNP surfaces first and purified with repeated centrifugation and suspension. Then excess UR and SP were mixed with UADD-AuNPs and the self-assembly of these components was carried out in buffer B2 by a heating and cooling process. The observation of good dispersion of nanoparticles and a slight UV-vis spectral shift (peak shift from 523 to 528 nm) of UADD-AuNPs in buffer suggest the attachment of UADD on the surface of AuNPs (Figure 3 and Figure S1†). The coverage of UADD on AuNPs was estimated by comparing the coverage of a fluorophore-labelled UADD (Alexa-UADD: 5' C6SS-CTC TCC CTC CCT CCC TCC C-Alexa 3') on AuNPs. It seems unlikely that the fluorophore attached to the opposite side (3'end) of the disulfide group (5' end) of UADD affects the immobilization. As expected, the UV-vis spectrum of Alexa-UADD-AuNPs almost overlaps that of UADD-AuNPs (Figure S2†). The fluorescence intensity of Alexa-UADD-AuNPs increased about 6.3 times (Figure S3†) after the addition of excess mercaptoacetic acid, suggesting that displacement of Alexa-UADD from the surface of AuNPs terminates the quenching of AuNPs. The coverage of Alexa-UADD on each AuNP was determined to be 48±2, which should be similar to the coverage of unlabelled UADD. As shown in Figure 3, the appearance of a weak peak at □260 nm on the spectrum in addition to a spectral shift indicates the hybridization of UR-SP to UADD-AuNPs because a large amount of nucleic acid bases were introduced upon the hybridization of UR-SP (21 bases + 71 bases) compared to only 19 bases on UADD. The coverage of UR-SP on UADD-AuNPs was determined to be 29±2 per particle using UV-vis and fluorescence spectroscopy. The hybridization efficiency of UR-SP to UADD-AuNPs is about 60% in this study.

We further investigated the fluorescence quenching effect from G-bases only in the case of UR-SP-UADD and the dual-quenching effect from G-bases and AuNPs in the system of UR-SP-UADD-AuNPs, respectively. As shown in Figure 4a and 4b, the formation of UR-SP1-UADD and UR-SP2-UADD after the hybridization of SP1 and SP2 to UR and UADD caused a drop in fluorescence intensity of UR to about 52% and 75%, respectively, mainly due to the fluorescence quenching from G-bases on the stem region of SP. In contrast, the self-assembly of UR-SP1 and UR-SP2 to UADD-AuNPs caused a decrease in fluorescence intensity to about 12% and 20%, respectively, mainly contributed by both the G-base quenching and the quenching from gold surfaces. This observation suggests that the introduction of the secondary quencher (AuNPs) enhanced the fluorescence quenching significantly and lowers the background signal dramatically. Thus, the dual-quencher system should improve the sensitivity and the detection limit.

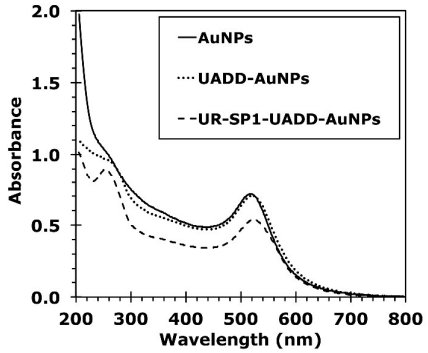

Figure 3. UV-vis absorption spectra of fresh AuNPs (10 nm diameter, 0.01 wt%, 5.7×10^{12} particles/mL ≈ 9.5×10^{-9} M), UADD-AuNPs, and UR-SP1-UADD-AuNPs.

We further investigated the detection of target sequences using the self-assembled biosensors UR-SP1-UADD-AuNPs and UR-SP2-UADD-AuNPs. Since temperature is very critical for DNA hybridization, as an example, the temperature profiles for fluorescence of UR, UR-SP, and UR-SP-UADD-AuNPs were investigated. As shown in Figure S4,† the fluorescence intensity of UR decreases as temperature increases due to the fluorescence quenching effect by solvent relaxation and this is a similar result to a previous study.[31] The fluorescence intensity of UR-SP2 increased as temperature increased from 20 to 48 °C due to the reduced quenching effect from G-bases when the closed SP2 undergoes a gradual opening process.

The intensity decreased as temperature increased from 48 to 76 °C due to the fluorescence quenching effect of solvent relaxation after SP2 completely changed to the open form. The transition temperature 48 °C is very close to the calculated melting temperature of SP (46.1 °C) shown in Table 1. Interestingly, UR-SP2-UADD-AuNPs shows a completely different temperature profile. The fluorescence intensity of UR-SP2-UADD-AuNPs increased as temperature increased from 20 to about 68 °C probably due to the continuously decrease of quenching from both G bases and AuNPs. Above 68 °C, the profile overlaps with UR, suggesting complete dehybridization of UR from SP, UADD, and AuNPs. Based on the temperature profiles, we conclude that a temperature below 48 °C will not cause dehybridization of UR-SP from UADD-AuNPs, and a temperature above 68 °C will cause significant dehybridization of UR, SP, and UADD-AuNPs. Thus for the detection of target sequences, 37 °C was selected for target incubation and 25 °C was used for collecting fluorescence spectra of samples.

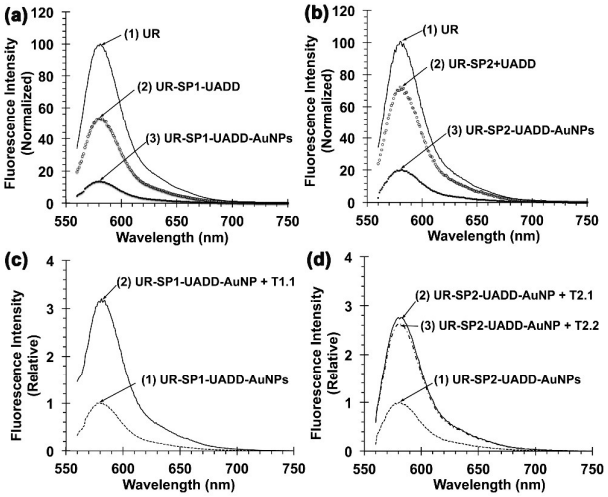

Figure 4. (a) Fluorescence spectra of (1) UR (5.0 nM), (2) UR-SP1-UADD (5.0 nM of UR, 5.5 nM of SP1, and 5.5 nM of UADD), and (3) UR-SP1-UADD-AuNPs (5.0 nM UR-SP1 hybridized to UADD-AuNPs) in PBS buffer B1 (pH 7.4, 137 mM NaCl, 5 mM Mg2+); (b) Fluorescence spectra of (1) UR (5.0 nM), (2) UR-SP2-UADD (5.0 nM of UR, 5.5 of nM SP2, and 5.5 nM of UADD), and (3) UR-SP2-UADD-AuNPs (5.0 nM of UR-SP2 on UADD-AuNPs) in PBS buffer B1; (c) Fluorescence spectra of (1) UR-SP1-UADD-AuNPs (5.0 nM UR-SP1 on UADD-AuNPs), (2) UR-SP1-UADD-AuNPs with 10.0 nM of target T1.1 in PBS buffer B1; (d) Fluorescence spectra of (1) UR-SP2-UADD-AuNPs (5.0 nM of UR-SP2 on UADD-AuNPs), (2) UR-SP2-UADD-AuNPs with 10.0 nM of target T2.1 in PBS buffer B1, and (3) UR-SP2-UADD-AuNPs with 10.0 nM of target T2.2 in PBS buffer B1. Fluorescence spectra were collected when samples were excited at 550 nm.

The time course to show the hybridization process of target T1.1 with UR-SP1-UADD-AuNPs (UR concentration: 5.0 nM) at 37 °C was further investigated. As shown in Figure S5,† in the absence of target sequences, fluorescence intensity remains almost the same over a period of 60 minutes. In contrast, the intensity increases gradually for all concentrations of target from 1 to 10 nM. An observable change of fluorescence intensity could be achieved even with a target concentration as low as 1.0 nM in as little as 5 minutes. A maximum 2.5 times increase in fluorescence intensity can be achieved after 60 minutes in the presence of 5 nM and 10 nM of target. A substantial increase can be achieved after 20 minutes incubation of target at 37 °C for all concentrations of target. Thus, an incubation time of 20 minutes at 37 °C was used for further investigation of the sensing ability of the self-assembled biosensors. As shown in 4c, the fluorescence intensity of UR-SP1-UADD-AuNPs (5.0 nM UR-SP1 on UADD-AuNPs) increased about 3.2 times after incubation with 2.0 equivalents of T1.1. In comparison, the fluorescence intensity of UR-SP2-UADD-AuNPs (5.0 nM UR-SP2 on UADD-AuNPs) increased about 2.7 and 2.6 times in the presence of 2.0 equivalents of T2.1 (a DNA target) and T2.2 (a microRNA target), respectively (Figure 4d). The slightly lower increase of fluorescence intensity in the case of SP2 compared to that of SP1 is probably due to the higher background signal of UR-SP2-UADD-AuNPs.

The titration curve and detection limit of target T1.1 using UR-SP1-UADD-AuNPs (5.0 nM UR-SP1 on UADD-AuNPs) in a micro-cuvette (50 µL) was demonstrated. As shown in Figure 5a, a considerable change can be observed in the presence of T1.1 as low as 0.01 picomoles (or 0.2 nM). A linear titration curve can be obtained in the range of 0 to 0.5 picomoles (or 0 to 10 nM). The selectivity of UR-SP1-UADD-AuNPs was further investigated. As shown in Figure 5b, the presence of a perfect DNA target sequence T1.1 or a microRNA target T1.4 enhanced the fluorescence intensity about 3 times. The target T1.2 matching the loop region and a single mismatch target T1.3 caused a lower increase in fluorescence intensity of about 2.3 and 2.0 times, respectively. As expected, a complete mismatch of target T1.5 did not cause a fluorescence intensity increase at all. This study suggests that the newly designed, self-assembled biosensor UR-SP-UADD-AuNPs can detect both DNA and microRNA target sequences, and a detection limit of 0.01 picomoles (or 0.2 nM) can be achieved.

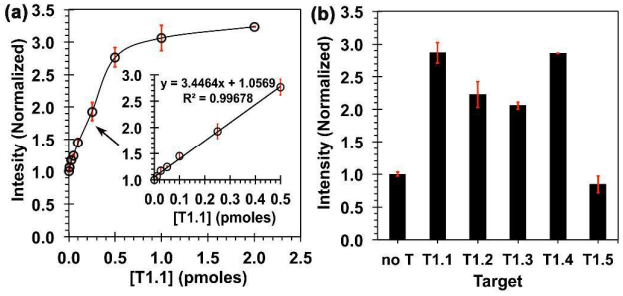

Figure 5. (a) A plot showing the changes of fluorescence intensity of UR-SP1-UADD-AuNPs in presence of target T1.1 of 0, 0.01, 0.025, 0.05, 0.1, 0.25, 0.5, 1.0, and 2.0 picomoles (or with a concentration of 0, 0.2, 0.5, 1.0, 2.0, 5.0, 10, 20, and 40 nM). Inset: a linear titration curve of UR-SP1-UADD-AuNPs in the presence of target T1.1 of 0, 0.01, 0.025, 0.05, 0.1, 0.25, and 0.5 picomoles (or 0, 0.2, 0.5, 1.0, 2.0, 5.0, and 10 nM) (b) Normalized fluorescence intensity of UR-SP1-UADD-AuNPs in the absence and in the presence of targets T1.1, T1.2, T1.3, T1.4, and T1.5.

Conclusions

In conclusion, we have developed a novel self-assembled biosensor for detecting unlabelled nucleic acids based on a modified SP with UR, and with the use of dual-quenchers. Compared to conventional molecular beacon-based biosensors, the use of universal reporters and universal addresses conjugated to AuNPs could avoid the very expensive covalent labelling process of a fluorophore and a quencher to two ends of an oligonucleotide stem-loop probe. More importantly, to construct MB based biosensors for many different target molecules, self-assembled biosensors with a universal reporter and a universal address could reduce the time of synthesis and the cost significantly. Furthermore the introduction of dual-quenchers (G bases and gold nanoparticles) could enhance the fluorescence quenching and reduce background signal, therefore enhancing the sensitivity to a detection limit of 0.01 picomoles (or 0.2 nM). This approach may be useful for the rapid, inexpensive, selective, and sensitive detection of unlabelled nucleic acids (DNAs and microRNAs).

Acknowledgements

We thank the Air Force Office of Scientific Research (FA9550-10-10343) for partial support of this research. SWTC thanks the support of the National Science Foundation. This publication was based on work supported by the NSF, while working at the Foundation. Any opinion, finding, and conclusions or recommendations expressed in this publication are those of the author and do not necessarily reflect the views of NSF.

References

1 D. Sidransky, *Science*, 1997, **278**, 1054.
2 X. Liu and W. Tan, *Anal. Chem.*,1999, **71**, 5054.
3 D. J. Cahill, *J. Immun. Meth.,* 2001, **250**, 81.
4 J. Wang, X. Cai, G. Rivas, H. Shiraishi, P. A. M. Farias and N. Dontha, *Anal. Chem.,* 1996, **68**, 2629.
5 G. Bonnet, S. Tyagi, A. Libchaber and F. R. Kramer, *Proc. Natl. Acad. Sci.*, 1999, **96**, 6171.
6 H. Kuhn, V. V. Demidov, J. M. Coull, M. J. Fiandaca, B. D. Gildea and F. M. D. Kamenetskii, *J. Am. Chem. Soc.,* 2002, **124**, 1097.
7 P. Zhang, T. Beck and W. Tan, *Angew. Chem. Int. Ed.*, 2001, **40**, 402.
8 J. Li, W. Zhou, X. Quyang, H. Yu, R. Yang, W. Tan, and J. Yuan, *Anal. Chem.*, 2011, **83**, 1356
9 S. Tyagi and F. R. Kramer, *Nat. Biotech.*, 1996, **14**, 303.
10 S. Tyagi, D. P. Bratu, and F. R. Kramer, *Nat. Biotech.*, 1998, **16**, 49.
11 J. A. Vet, A. R. Majithia, S. Tyagi, S. Dube, B. J. Poiesz and F. R. Kramer, *Proc. Natl. Acad. Sci*., 1999, **96**, 6394.
12 D. P. Bratu, B. Cha, M. M. Mhlanga, F. R. Kramer and S. Tyagi, *Proc. Natl. Acad. Sci*., 2003, **100**, 13308.
13 P. Sheng, Z. Yang, Y. Kim, Y. Wu, W. Tan and S. A. Benner, *Chem. Commun.,* 2008, 5128
14 X. Tan, W. Chen, S. Lu, Z. Zhu, T. Chen, G. Zhu, M. You and W. Tan, *Anal. Chem.* 2012, **84**, 8272
15 K. Huang, A. Angel and A. Marti, *Anal. Bioanal. Chem.*, 2012, **402**, 3091.
16 D. J. Maxwell, R. Taylor and S. Nie, *J Am. Chem. Soc.*, 2002, **124**, 9606
17 X. Mao, H. Xu, Q. Zeng, L. Zeng and G. Liu, *Chem. Commun.* 2009, 3065
18 Y. He, K. Zeng, A. Gurung, M. Baloda, H. Xu, X. Zhang and G. Liu, *Anal Chem.* 2010, **82**, 7169
19 H. Peng, C. M. Strohsahl, K. E. Leach, T. D. Krauss and B. L. Miller, *ACS Nano* 2009, **3**, 2265.
20 R. Yang, J. Jin, Y. Chen, N. Shao, H. Kang, Z. Xiao, Z. Tang, Y. Wu, Z. Zhu and W. Tan, *J. Am. Chem. Soc.,* 2008, **130**, 8351.
21 C. Lu, J. Li, J. Liu, H. Yang, X. Chen and G. Chen, *Chem. Eur. J.*, 2010, **16**, 4889.
22 F. R. Baptista, S. A. Belhout, S. Giordani and S. J. Quinn, *Chem. Soc. Rev.,* 2015, **44**, 4433.
23 M. Torimura, S. Kurata, K. Yamada, T. Yokomaku, Y. Kamagata, T. Kanagawa and R. Kurane, *Anal. Sci.*, 2001, **17**, 155.
24 I. Nazarenko, R. Pires, B. Lowe, M. Obaidy and A. Rashtchian, *Nucleic Acids Res.,* 2002, **30**, 2089.
25 B. Dubertret, M. Calame and A. J. Libchaber, *Nat. Biotech.,* 2001, **19**, 365.
26 H. Wang, J. Li, Y. Wang, J. Jin, R. Yang, K. Wang, and W. Tan, *Anal. Chem.,* 2010, **82**, 7684.
27 J. A. Dougan, C. Karlsson, W. E. Smith and D. Graham, *Nucleic Acids Res.*, 2007, **35**, 3668.
28 L. Demers, C. A. Mirkin, R. Mucic, R. Reynolds, R. L. Letsinger, R. Elghanian and G. Viswanadham, *Anal. Chem.,* 2000, **72**, 5535.
29 F. Borriello, J. Oliveros, G. J. Freeman, L. M. Nadler and A. H. Sharpe, *J. Immunol*., 1995, **155**, 5490.
30 Perry, M. M.; Moschos, S. A.; Williams, A. E.; Shepherd, N. J; Larner-Svensson, H. M.; Lindsay, M. A. *J. Immunol.*, 2008, **180**, 5689.
31 S. -W. Tam-Chang, T. D. Carson, L. Huang, N. G. Publicover and K. W. Hunter, Jr., *Anal. Biochem*., 2007, **326**, 126.